

## Article

# Innovative Solutions for the Rehabilitation of Bridges Using Flexible Galvanized Steel Structures: A Case Study

Doina Negrea <sup>1,\*</sup>, Christiana Emilia Cazacu <sup>2</sup> and Mircea Conțiu <sup>2,\*</sup><sup>1</sup> Viacon Romania SRL, 507165 Prejmer, Romania<sup>2</sup> Civil Engineering Department, Faculty of Civil Engineering, Transilvania University of Braşov, 500152 Braşov, Romania; cazacu.christiana@unitbv.ro

\* Correspondence: doina.negrea@viacon.ro (D.N.); mircea.contiu@unitbv.ro (M.C.)

**Abstract:** The objective of the project was the rehabilitation and expansion of one bridge, located on the DN28 (a national road) in Sarca, Iasi County. The solution includes an atypical use of the flexible galvanized steel structure. The main challenge in this case was to finish the works without any traffic interruption on this section of the national road, as well as the assembly of the said corrugated steel structure under the existing bridge. The work was executed in record time and with reduced costs in comparison with the classic alternative solutions, such as concrete bridges. The paper highlights practical aspects from the key moments of the project and presents the major challenges and how they were solved for both the design and the construction stages.

**Keywords:** flexible steel structures; buried steel bridge; corrugated steel plates; bridge repair; bridge retrofit; rehabilitation



**Citation:** Negrea, D.; Cazacu, C.E.; Conțiu, M. Innovative Solutions for the Rehabilitation of Bridges Using Flexible Galvanized Steel Structures: A Case Study. *Sustainability* **2023**, *15*, 6200. <https://doi.org/10.3390/su15076200>

Academic Editor: Constantin Chalioris

Received: 5 February 2023

Revised: 30 March 2023

Accepted: 31 March 2023

Published: 4 April 2023



**Copyright:** © 2023 by the authors. Licensee MDPI, Basel, Switzerland. This article is an open access article distributed under the terms and conditions of the Creative Commons Attribution (CC BY) license (<https://creativecommons.org/licenses/by/4.0/>).

## 1. Introduction

Ever since Roman times, the arch has been highlighted as one of the most efficient structural systems, combining a very rational use of materials with a suitable structural behavior and pleasing aesthetics. A testament to the durability and structural robustness of arch structural systems are the numerous roman arches still standing today. Although romans used masonry and wood for the construction of bridges, only the masonry bridges survived, such as the bridge over the Tagus River in Alcantara, Spain which is almost 2000 years old [1].

Today's bridge solutions make use of modern materials, such as concrete and steel which are continuously developed and improved. This allowed the design to reach superior slenderness, decreasing the cross-section size and, implicitly, the material quantities even further.

Modern arch bridges are typically reserved for medium-to-long span bridges. Concrete arch bridges are recommended in the 50–400 m span range, while steel arches can even reach spans of 600 m [2]. Recently, buried arch bridges have also been used for small span as an alternative to traditional bridge solutions. Concrete and steel solutions may be applied.

The buried concrete arch bridges are perfectly suited to prefabrication due to their small element sizes and weights, which makes them a very attractive solution for small spans. Various systems (e.g., BEBO Beton Bogen, NUCON, Flexi-Arch, Pearl-Chain concrete arch bridge, PCASO precast concrete buried arch bridge with steel outriggers) have been designed and built [3–7]. Detailed studies on their structural behavior have also been conducted, with measurements on in-service structures [4,6,8–10].

Flexible steel structures, made from thin corrugated steel plates, constitute an efficient alternative to traditional bridges and culverts [11,12]. This solution has been in use since the 1960s [13] due to its reduced price and construction time [14]. Studies on deterioration

mechanisms, service life estimation and rehabilitation approaches consolidated their application as efficient infrastructure solution and proved that a service life of 100 years could be reached through the application of adequate coating systems [15–17].

The corrugated steel structure itself is extremely flexible and is only able to handle the design loads (its self-weight, that of the soil fill and live loads) due to the interaction with the surrounding soil, which makes the compression around the structure redistribute to a uniform ring [18]. This theory remains at the basis of the design for this type of structures even today and is included in most norms and specifications [19] such as AASHTO LRFD Bridge Design Specifications [20] or the Ontario Highway Bridge Design Code (OHBDC) [21].

The problem of the soil-structure interaction has been extensively studied, using both theoretical models and full-scale tests. The execution of the backfill is carried out in small steps and represents, probably when the structure is at its weakest and most vulnerable. Several studies [22–24] focus precisely on that. The behavior of the finished structure under static traffic loads has been evaluated in multiple studies [25–27], while fewer considered dynamic loads [28–32].

This kind of structure proved to be so efficient that applications in other areas, such as tunnels [33,34] and in retrofitting existing bridges, were considered, extending them way beyond their original scope.

As sustainability has become one of the main goals of our society today, a spotlight has been pointed at the construction industry, which, according to United Nations Environment Program, is estimated to generate 39% of the world's gross annual carbon emissions. As the population of the planet continues to rise, there is no real way to stop the continued growth of the construction sector. Thus, focus has been shifted towards researching and applying environmentally friendly solutions. In comparison with the concrete bridge solutions that are typically used for the 2–25 m span range, the corrugated flexible steel structures offer the same functionality (load bearing capacity, life span, etc.), but with a reduced carbon footprint due to the more environmentally friendly material (steel) and the reduced quantities (the structure is made out of thin corrugated steel plates). In this solution, concrete may be used for the foundations, which are only required for spans larger than 8–10 m.

The demolition and reconstruction of old structures uses a massive amount of raw materials and energy, generating a very large carbon footprint. The much greener approach of repair and retrofit of existing structures has become a real trend today in the construction sector. This reduces the carbon footprint by a large factor, as only minimalist demolition works and fewer raw materials are required. By applying an environmentally friendly solution, the carbon footprint is reduced even further.

This paper describes in detail a retrofit and extension solution for an existing concrete bridge using a flexible galvanized steel structure, which generated only minimal traffic restrictions. It includes practical aspects, presents the major challenges and how they were solved both in the design and construction stages of the project. In comparison with the replacement of the bridge with a new one, the carbon footprint is significantly reduced by retrofitting the existing structure and applying an environmentally friendly solution.

## 2. Status of the Bridge before the Construction Works

National road DN28 connects some of the main cities from north-eastern Romania (Iasi and Roman) and continues up to the border with the Republic of Moldova at Albița. A typical section of the road comprises two 3.50 m wide lanes and a 2.50 m wide shoulders on each side, resulting in a total width of 12.00 m.

The bridge being studied is located on national road DN28 near Sarca village in Iasi County. It crosses the Valea Oii stream with a span of 10 m. The carriageway over the bridge has a width of 7.50 m and has 1.20 m wide sidewalks on both sides, adding up to a total width of the superstructure of 10.70 m. A photograph of the existing bridge at the start of the construction works is presented below, in Figure 1.



**Figure 1.** The existing bridge at the start of the construction works.

The superstructure is a simply supported single-span cast-in-place reinforced concrete slab with a height of 65 cm and a width of 9.10 m; the 80 cm cantilevers are present along the whole bridge, on both sides of the slab.

The bridge dates back to 1959 and the superstructure has already been subjected to a strengthening operation in 2001, through the execution of a 12 cm over-concreting slab.

The superstructure is supported on both ends by reinforced concrete wall abutments with back and wing walls and spread footings at a depth of around 3.50 m.

As its designed life span of 50 years had already expired, the existing structure was in poor shape; however, it did not show any signs of critical structural damage or failure. This means that the application of a repair and strengthening solution would also be possible.

The main issue of the structure was its reduced width compared to that of the road before and after the bridge. This generated a major road safety hazard as cars driving at around 90 km/h on a 12.00 m wide carriageway would abruptly meet a reduced 7.80 m wide carriageway, limited on both sides by large vehicle restraints systems. The road administrator decided it was time to correct this dangerous situation by extending the structure on both sides, thus obtaining a constant road width of at least 12.00 m across the bridge. The necessary works need to be carried out with minimal interruption of traffic on the national road.

### 3. Analysis of Solutions

For this situation, the following two solutions are typical:

- Strengthening/extending the existing structure;
- Execution of a complete/partial new bridge after the total/partial demolition of the existing structure;

The strengthening and extension of the existing structure may only be applied where the structure is still in good condition, which is not the case here. The presence of cracks in the superstructure and the peeling of the concrete cover layer left the reinforcement unprotected, which, in turn, started to rust. This complicated the strengthening solution even more. The increased difficulty and the typical life span of 15 years of a strengthening solution eliminated it from the list of viable options.

Normally, the next natural choice would be to demolish and rebuild a new superstructure on repaired and strengthened abutments. This would allow the bridge, which would practically be almost new, to reach a lifespan of 100 years. This solution, however, has two main drawbacks: the large costs generated by demolishing the existing structure and building a new one and the fact that the traffic would be interrupted or seriously affected for quite a long time, which could reach a period of time even longer than a whole year.

For this situation, a third solution has been devised: with the use of a corrugated steel structure that will be placed below the existing bridge, the rehabilitation works could be finished without any interruption of traffic. This solution will be detailed below.

### 3.1. Innovative Solution Using a Flexible Galvanized Steel Structure

The third solution is a retrofit and widening of the bridge by using a galvanized corrugated steel structure. This is actually the solution that was applied and the resulting bridge is presented in Figure 2.



Figure 2. The finalized bridge.

The cross-section and longitudinal sections presented in Figures 3 and 4 highlight the main characteristics of this solution:

- the galvanized corrugated steel structure is placed below the superstructure of the existing bridge, which will not be removed and will be embedded in the final structure;
- the superstructure is extended on both sides by 3.60 m/2.50 m.

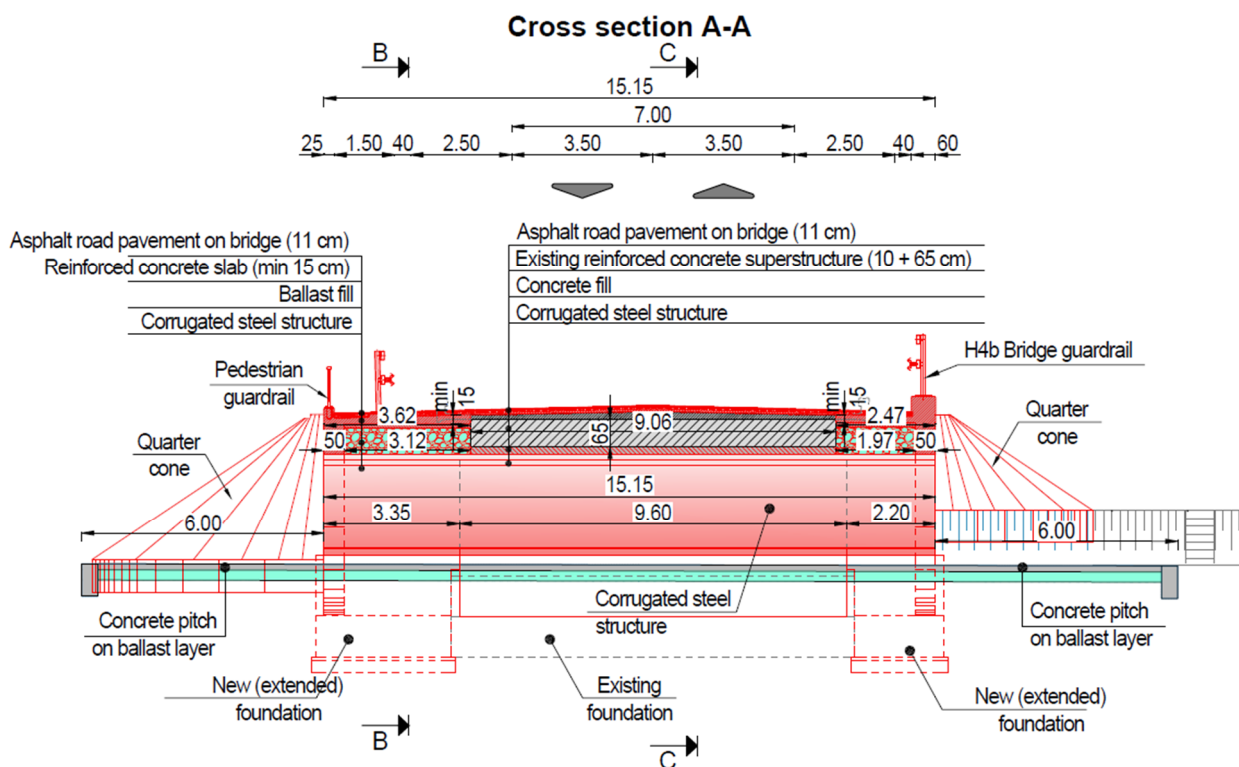


Figure 3. Cross section of the galvanized corrugated steel structure retrofit solution.

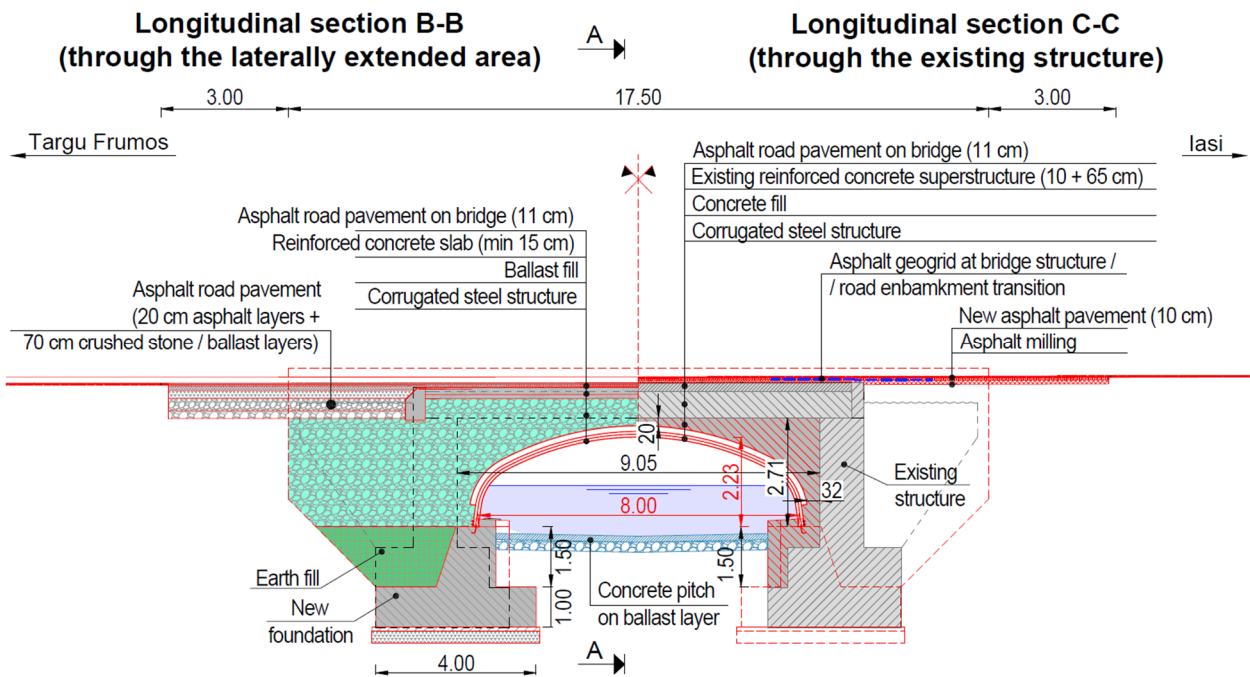


Figure 4. Longitudinal sections of the galvanized corrugated steel structure retrofit solution.

As one of the main requirements of the project was to carry out the necessary works without interrupting of traffic over the bridge, the superstructure was not demolished. The biggest profile that fits the available space inside the existing bridge of approximately  $9.00 \times 2.70$  m is the Viacon Supercor SB-8L, presented in Figure 5. For the whole upper part of the arch, stiffener ribs are alternatively placed which produces a closed double-loop section. The steel grade S355MC is used.

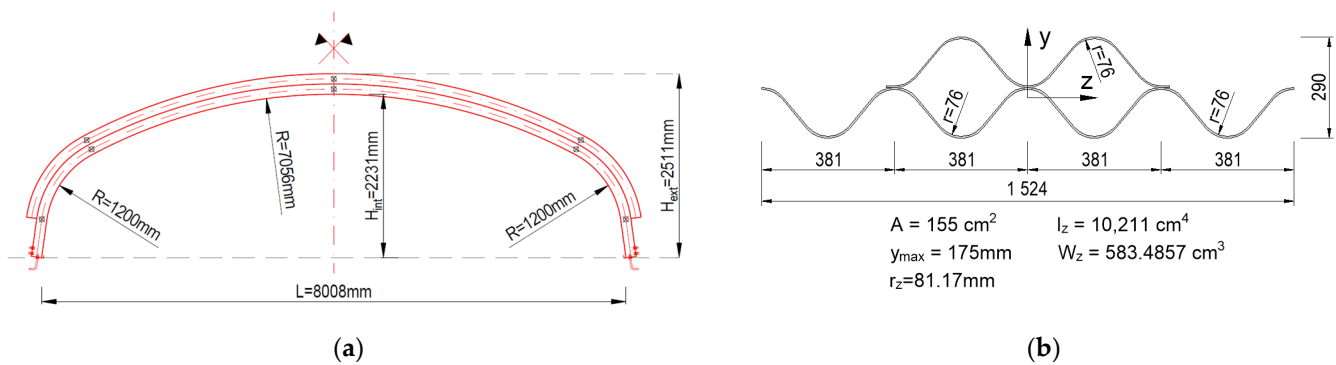


Figure 5. Details of the corrugated steel structure. (a) Elevation view. (b) Corrugated profile cross-section.

The remaining width of the superstructure after the demolition of the transverse sidewalk cantilevers was of approximately 9.06 m. The flexible steel structure needed to be wider (Figure 6) as the new bridge, compared to the old one, had an extended carriageway and a total width of 15.15 m.



**Figure 6.** Aerial view highlighting the difference in width between the existing bridge and the flexible steel structure.

A couple of photographs from the assembly and execution of the steel structure itself are presented below in Figure 7.



**Figure 7.** Photographs from the assembly process.

In order to minimize transport costs, the steel structure arrived in packages containing stacked segments and the necessary materials for the assembly of the structure: fasteners, anchor screws, base channels, an assembly kit, an assembly drawing, and additional instructions. All work needs to be carried out very carefully to avoid damaging the corrosion protection of the steel structure, which had already been applied in the factory.

One of the main challenges of the assembly process was the very limited space available between the steel structure and the existing concrete bridge, where a worker could not fit. The solution was to incrementally assemble the structure on one side of the existing bridge and then slide it into position.

The connection to the foundation is accommodated with the help of a base channel bolted to the steel structure on one side and the foundation on the other side. For the latter, anchor bolts embedded in the concrete are used. A detail is presented below in Figure 8. In this case, the base channel also provided the “track” for the sliding process of the assembled steel structure.

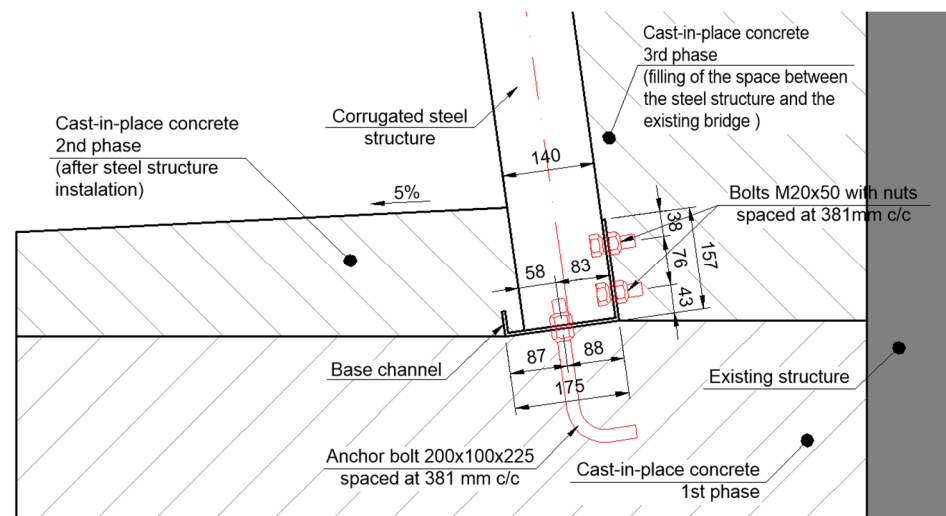


**Figure 8.** Detail of the steel structure connected with the foundation.

After assembly, at least 5% of the total number of bolts should be checked with a torque wrench. Inspection is carried out on randomly selected bolts, evenly located around the structure. A photograph of the fully assembled steel structure is presented in Figure 9.



**Figure 9.** Steel structure connected with the foundation.

The typical solution for this type of flexible steel bridge is to make a high-quality ballast or crushed stone fill around it.

Because a superior compaction level of Proctor 95% has to be reached for the earth fill and the steel structure is prone to buckling, the fill should be symmetrically executed in small steps of around 30 cm. The earth fill around the structure will interact with the flexible steel structure at every step of the construction process, offering lateral support and reducing the risk of buckling.

This solution cannot be applied under the existing bridge because there is no way to reach the necessary compaction level. That is why the space between the existing bridge and the flexible steel structure was filled with concrete.

On both sides of the existing structure, the high-quality earth fill has a width of about 2.00/3.00 m and is limited by a headwall, that is anchored both in the foundation and the steel structure itself. Figure 10 shows the space between the existing structure and the headwall.



**Figure 10.** View of the steel structure extended beyond the width of the existing concrete bridge and of the formwork for the headwall.

Another issue of the bridge repair and extension concept is the large difference in stiffness between the original concrete structure and the earth fill, in the transverse direction. This kind of difference would result in settlements of the earth filling over long periods of time, especially because the compaction level is hard to reach due to the very limited space available.

To solve this, a 15 cm thick reinforced concrete slab has been executed above the earth fill. The slab has a robust structural connection to the existing structure and the headwall and ensured the road traffic experiences a similar stiffness to that of the original structure.

At both abutments, the back wall is extended in the transverse direction using a concrete block, which will be embedded in the earth fill. The concrete block will act as an end support for the reinforced concrete slab and ensures the transition between the two different road pavements: the one above the bridge slab and the one over the embankment.

The last step in the construction process is the execution of the road pavement and the installation of road safety equipment. Figure 11 shows the final extended road section along the length of the bridge, after the end of the construction process and the restart of traffic.



**Figure 11.** Global view of the bridge from the road surface.

### 3.2. Design of the Flexible Steel Structure

Typically, a high-quality ballast or crushed stone fill would be executed around this type of flexible structure and would interact with it offering lateral support and reducing the risk of buckling.

In this situation, the execution of the concrete fill between the steel structure and the existing bridge creates a unique loading situation for the first one: the resulting forces from the self-weight of the steel and of the fresh concrete will act solely on the steel structure, without the usual additional support from the interacting earth fill. After hardening, the resulting concrete structure above the corrugated steel arch will be very stiff and will not transfer loads to the flexible steel structure up to a point that may generate any kind of relevant response.

As this is the only relevant design case, an evaluation of pressure acting on the structure at the concrete-pouring stage needed to be carried out. The flexible steel structure actually acts as formwork; therefore, the design should follow the corresponding regulations. Thus, the approach from ACI 347R-14 "Guide to formwork for concrete" [35] will be applied.

The document provides clear guidelines for the evaluation of loads, which are divided into vertical and lateral pressure. Even though the steel structure is quite different from the typical formwork structures that the norm was made for, it still offers the closest applicable description of the concrete pressures generated during the pour and settling. In order to account for those differences, some adaptations are necessary.

For the fresh concrete pour design case, no live loads need to be considered on the steel structure due to the very small space between the structures, which does not allow anything to be inserted at the time on concrete pouring.

When considering that the fresh concrete acts such as a fluid, it generates hydrostatic pressure, as shown in the following formula:

$$p = \rho gh \text{ [kPa]} \quad (1)$$

where

$p$ —hydrostatic pressure [kPa];

$\rho = 2.4 \text{ t/m}^3$  — density of fresh concrete;

$g = 9.81 \text{ m/s}^2$  — gravitational constant;

$h$ —depth of fluid concrete from the top of the pour to considered level [m].

If the concrete is poured rapidly, no settling of the aggregates or stiffening of the concrete paste can take place and the lateral pressure will be equal to the hydrostatic pressure. If the rate of concrete pouring is sufficiently small, some stiffening of the concrete will take place before the pour is finished due to the settling of the aggregates and the stiffening of the concrete mix itself, leading to a reduction in the horizontal pressure on the formwork. This is similar in behavior to that of soil: the concrete starts to exhibit internal friction between the aggregates and cohesion due to the stiffening of the concrete paste. Thus, the lateral pressure will be taken as the hydrostatic pressure up to a certain depth limit, which will be defined below, and will have a reduced value from that point onward.

ACI 347R-14 estimates the maximum lateral pressure of fresh concrete for two cases: columns and walls. Between the two, the wall fits the behavior of the concrete pour on the flexible steel structure better, as it is defined as "vertical elements with at least one plan dimension greater than 2 m". The presented formulas may be applied for concrete with a slump of less than 175 mm and is placed with normal internal vibration to a depth of less than 1.2 m. [35]

For walls with a rate of placement of less than 2.1 m/h and a placement height of less than 4.2 m, the maximum lateral pressure from the fresh concrete is equal to:

$$p_{max} = C_w C_C \left[ 7.2 + \frac{785R}{T + 17.8} \right] = 33.52 \text{ kPa} \quad (2)$$

where

$C_w = 1.00$  (for density of concrete between 2240 and 2400 kg/m<sup>3</sup>) – unit weight coefficient;

$C_C = 1.00$  (for cement types I, II and III without retarders) – chemistry coefficient;

$R = 1.1$  m/h – rate of concrete pour;

$T = 15$  °C – temperature of concrete during placing.

The hydrostatic pressure always acts normal in relation to the surface and the lateral pressure may only be applied to vertical surfaces (Figure 12). The flexible steel structure has an arch shape, which means that the contact surface has a constant variation along the whole span. As the lateral pressure completely replaces the hydrostatic pressure for vertical surfaces and the lateral pressure for horizontal surfaces is null, a weighted average between the two will be applied to the inclined surface, based on the angle of slope  $\alpha$ :

$$p_{slope} = p \cdot [\cos(\alpha)]^2 + p_{max, norm} \cdot [\sin(\alpha)]^2 \quad (3)$$

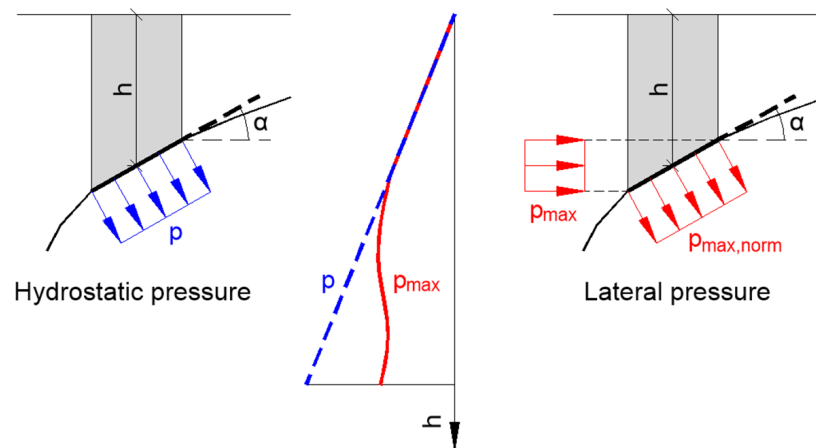


**Figure 12.** Hydrostatic/lateral pressures acting on inclined surfaces.

The relationship between hydrostatic pressure and lateral pressure with the variation of the angle of slope  $\alpha$ , generated using Equation (3), is represented in Figure 13:

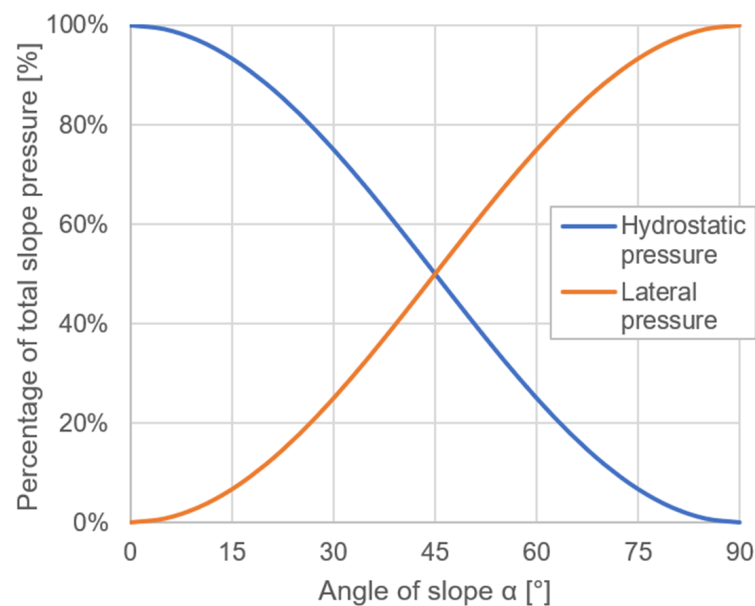


**Figure 13.** Composition of total slope pressure, based on angle of slope.

The structure itself is a double-pinned arch. Due to its particularities (overall shape and variation of the cross section) and those of the loading (as calculated below), a finite element analysis is necessary. From the very large FEM software pool currently available, CSiBridge has been chosen as it can be tailored to bridge systems and offers the required functionalities for this study.

As the loading due to the weight of the fresh concrete is constant along the middle of the structure, the behavior of the structure will also be constant. In this case, a 2D model containing a strip of the structure will exhibit the correct structural behavior and provide the relevant response, while keeping the model sufficiently simple, the analysis time short and the results easy to interpret. Before loading with the earth fill, the edges of the steel structure are stiffened by the headwalls. Loading the two edge strips with the earth fill weight will not generate an important response in the steel structure, as the head walls, due to their high stiffness, will absorb the loads almost completely.

Thus, a 2-dimensional model containing a strip of the structure from the sector loaded by the fresh concrete pressures will suffice. This is in line with the typical design approaches for this type of structures. An overview of the 2D model of the middle strip is represented in Figure 14. In order to closely model the varying curvature of the arch structure, a discretization of 30 elements has been applied, with varying lengths (larger element sizes are used near the crown and smaller ones closer to springs).

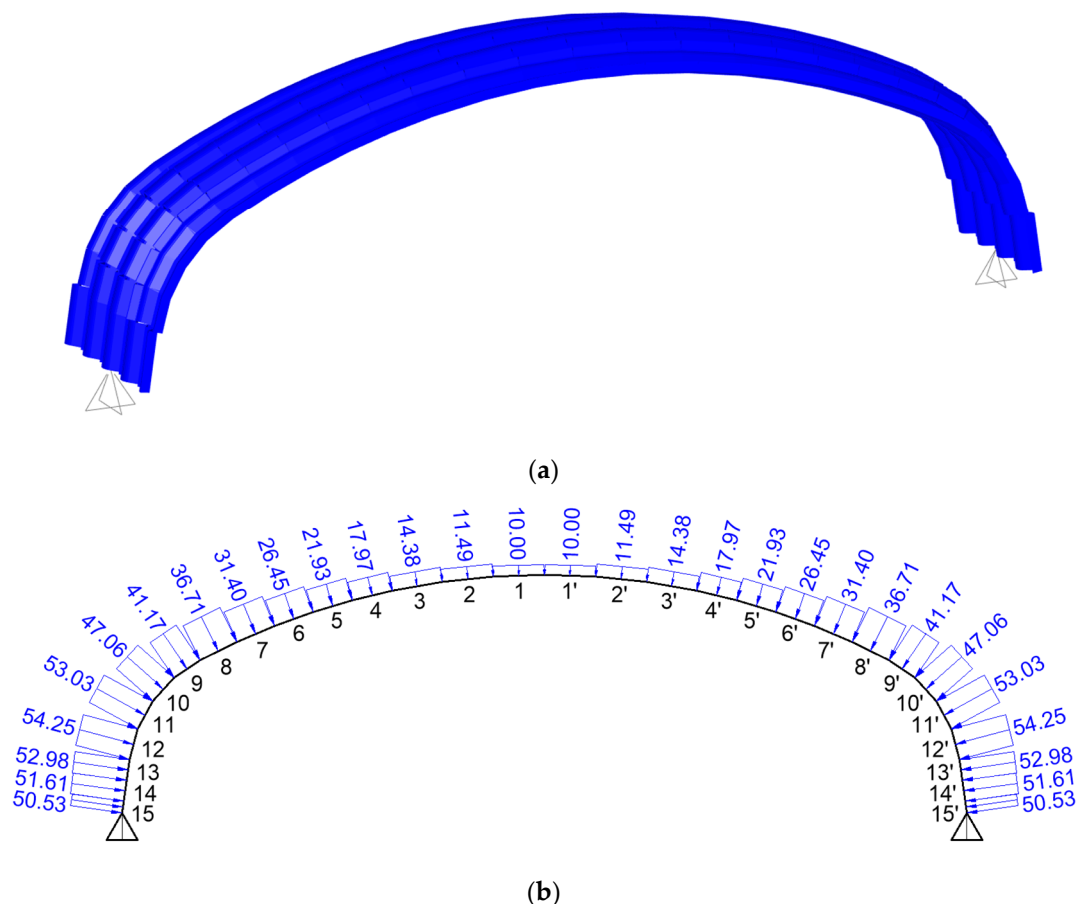


**Figure 14.** Finite element model. (a) Overview. (b) Applied fresh concrete pressures.

For each beam element from the arch model, the pressure is calculated according to the methodology described above. The resulting values are presented in Table 1.

Furthermore, because the concrete will be injected, especially for the upper portion, where it comes in contact with the existing bridge's superstructure, an increase in pressure may occur. This effect is taken into account by increasing the pressure by a factor of 2.00

for the upper portion, where the concrete is fresh, and going down to a factor of 1.50 at the bottom, where the concrete has partially set and exhibits some stiffening already. The resulting values are presented in Table 2.

**Table 1.** Pressures acting on the structure due to the self-weight of the fresh concrete.

No.	$\alpha$ [deg]	h [m]	Hydrostatic Pressure		Lateral Pressure			Total Pressure	
			p [kPa]	$[\cos(\alpha)]^2$ [%]	$P_{\max}$ [kPa]	$\sin(\alpha)$	$P_{\max, \text{norm}}$ [kPa]	$[\sin(\alpha)]^2$ [%]	$P_{\text{slope}}$ [kPa]
1/1'	1.98	0.21	5.00	99.9%	5.00	0.035	0.17	0.1%	5.00
2/2'	5.95	0.24	5.82	98.9%	5.82	0.104	0.60	1.1%	5.77
3/3'	9.92	0.31	7.46	97.0%	7.46	0.172	1.29	3.0%	7.28
4/4'	13.49	0.40	9.58	94.6%	9.58	0.233	2.24	5.4%	9.18
5/5'	16.67	0.50	12.05	91.8%	12.05	0.287	3.46	8.2%	11.34
6/6'	19.84	0.63	15.02	88.5%	15.02	0.339	5.10	11.5%	13.87
7/7'	23.02	0.77	18.48	84.7%	18.48	0.391	7.22	15.3%	16.75
8/8'	26.19	0.93	22.42	80.5%	19.17	0.441	8.46	19.5%	19.98
9/9'	33.93	1.11	26.55	68.8%	19.17	0.558	10.70	31.2%	22.89
10/10'	47.68	1.30	31.28	45.3%	19.17	0.739	14.17	54.7%	26.82
11/11'	61.43	1.55	37.19	22.9%	19.17	0.878	16.83	77.1%	31.21
12/12'	75.18	1.83	43.92	6.5%	19.17	0.967	18.53	93.5%	33.16
13/13'	82.06	2.08	49.86	1.9%	19.17	0.990	18.98	98.1%	33.52
14/14'	82.06	2.28	54.69	1.9%	19.17	0.990	18.98	98.1%	33.61
15/15'	82.06	2.44	58.45	1.9%	19.17	0.990	18.98	98.1%	33.69

**Table 2.** Increase in fresh concrete pressures due to execution technology (injection).

No.	h [m]	Total Slope Pressure $P_{\text{slope}}$ [kPa]	Pressure Increase due to Injection of Concrete	
			Factor	Increased Pressure
			f	P [kPa]
1	0.21	5.00	2.00	10.00
2	0.24	5.77	1.99	11.49
3	0.31	7.28	1.98	14.38
4	0.40	9.18	1.96	17.97
5	0.50	11.34	1.93	21.93
6	0.63	13.87	1.91	26.45
7	0.77	16.75	1.87	31.40
8	0.93	19.98	1.84	36.71
9	1.11	22.89	1.80	41.17
10	1.30	26.82	1.75	47.06
11	1.55	31.21	1.70	53.03
12	1.83	33.16	1.64	54.25
13	2.08	33.52	1.58	52.98
14	2.28	33.61	1.54	51.61
15	2.44	33.69	1.50	50.53

The graphic representation of the values from Tables 1 and 2 is shown below, in Figure 15. It highlights the reduction in loads due to the stiffening of the concrete during the pour procedure and the increase in pressure caused by the injection execution.

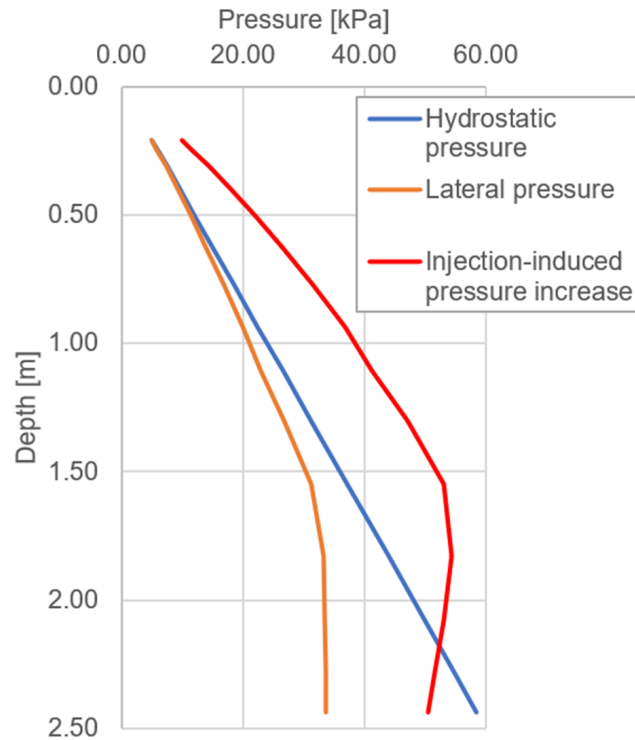


Figure 15. Evolution of pressures with depth.

These pressures are applied to the finite element model, as shown in Figure 14b.

After the concrete hardens, it forms a stiff arch structure that will absorb most of the traffic loads. As the steel structure is quite flexible, it requires larger deformations than the concrete arch is capable of to be loaded to a significant point. Furthermore, as no connection between the concrete and the steel structure is made, the latter will remain almost completely unloaded. This also holds true for both ends of the steel structures, where the slab on top of the earth fill will distribute the loads between the existing structure and the still head wall, leaving the flexible steel structure almost completely unloaded, again. The only relevant loads that the steel structure is actually subjected to are its self-weight and the weight of the fresh concrete.

The ULS frame forces are shown in the diagrams below in Figure 16. The model has the width of 1.524 m, equal to that of the cross-section from Figure 5b.

For the definition of the cross-section class, the steel profile may be considered equivalent to that of a round pipe with a 290 mm diameter and medium thickness of 5 mm. According to Eurocode 3, the cross-section is of class 3, as shown in Equation (4) [36]. All the following structural checks will consider elastic behavior.

$$\text{For class 3: } d/t = 290 \text{ mm}/5 \text{ mm} = 58 \leq 59.05 = 90 \cdot 0.81^2 = 90\varepsilon^2 \quad (4)$$

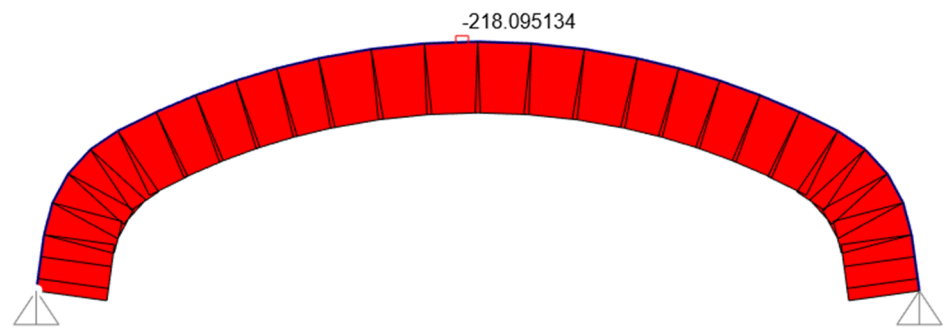
where  $\varepsilon = \sqrt{235/f_y} = \sqrt{235/355} = 0.81$ .

As the steel structure is subjected to compression and is quite flexible, it will be liable to flexural buckling. The critical buckling force was calculated through the methodology from EN 1993-2 Annex D [37]. The buckling behavior of the structure can be equated

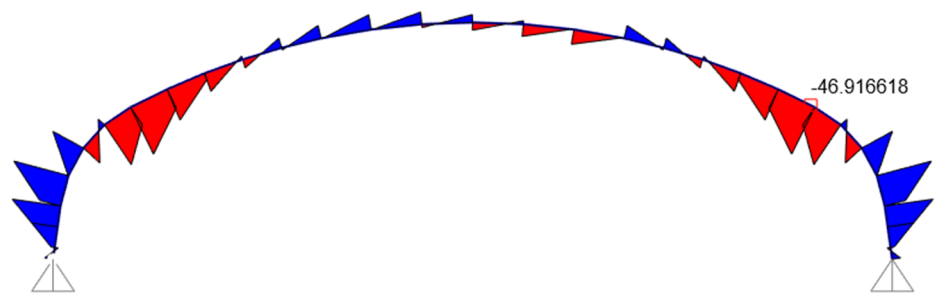
with in-plane buckling of double-pinned circular arches. For simplification, the stiffened cross-section was considered to be constant along the whole length of the arch.

$$\frac{f}{l} = \frac{2.23}{8.00} = 0.28 \rightarrow \beta = 1.05$$

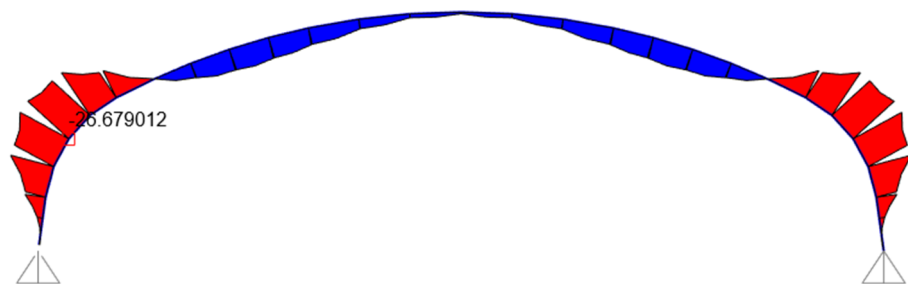
$$N_{cr,EC3} = \left(\frac{\pi}{\beta_s}\right)^2 EI_y = \left(\frac{\pi}{1.05 \cdot 5.1 \text{ m}}\right)^2 210 \text{ GPa} \cdot 10211 \text{ cm}^4 = 6508 \text{ kN} \quad (5)$$



(a) Axial force diagram [kN]



(b) Shear force diagram [kN]



(c) Bending moment diagram [kNm]

**Figure 16.** Design frame forces.

Due to the complex shape of the structure and the variation of the cross-section along the length of the arch, an eigenvalue buckling analysis has been carried out on the finite element model. The buckling shape is presented below, in Figure 17.

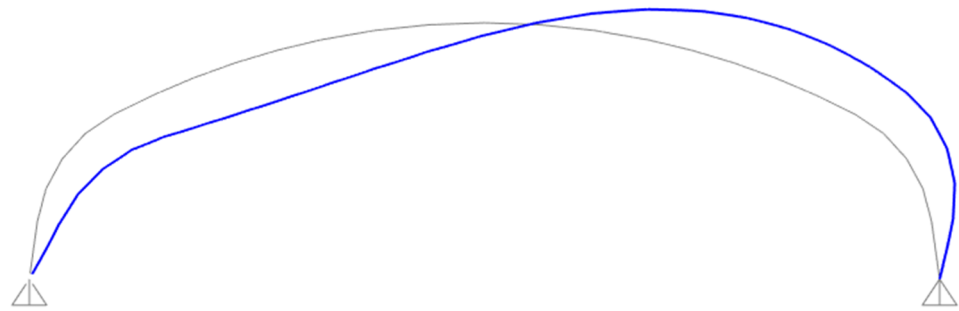


**Figure 17.** First buckling mode—factor 56.95.

The resulting critical buckling force, generated from the 2D FEM model, is:

$$N_{cr,FEM} = 110.05 \text{ kN} \cdot 56.95 = 6267 \text{ kN} \quad (6)$$

Between the two values, the one from the FEM model will be used in the structural checks, as it considers the exact shape of the structure, the variation of the cross-section and it is less favorable.

The reduction factor  $\chi$  is evaluated below, in Equation (7) [36].

$$\bar{\lambda} = \sqrt{\frac{Af_y}{N_{cr}}} = \sqrt{\frac{155 \text{ cm}^2 \cdot 355 \text{ MPa}}{6267 \text{ kN}}} = 0.937$$

$$\alpha = 0.49 \text{ (imperfection factor, conservatively taken for buckling curve C)}$$

$$\Phi = 0.5 \left[ 1 + \alpha (\bar{\lambda} - 0.2) + \bar{\lambda}^2 \right] = 0.5 [1 + 0.49 \cdot (0.937 - 0.2) + 0.937^2] = 1.1195 \quad (7)$$

$$\chi = \frac{1}{\Phi + \sqrt{\Phi^2 - \bar{\lambda}^2}} = \frac{1}{1.1195 + \sqrt{1.1195^2 - 0.49^2}} = 0.5773$$

The ultimate limit-state resistance check with and without buckling is presented below [36]. The resulting shear force is very small and does not need to be considered separately in the design.

Because the injection of the fresh concrete is a highly dynamic procedure that cannot be thoroughly controlled and to keep in accordance with typical formwork design regulations (the steel structure acts as formwork without additional supports for the fresh concrete), an additional safety factor  $\gamma_{frm} = 2.00$  will be added.

$$\frac{N_{Ed}}{\gamma_{M0} \cdot \gamma_{frm} \cdot Af_y} + \frac{M_{Ed}}{\gamma_{M0} \cdot \gamma_{frm} \cdot W_{el,min} f_y} = \frac{-218.10 \text{ kN}}{1.00 \cdot 2.00 \cdot 155 \text{ cm}^2 \cdot 355 \text{ MPa}} + \frac{-26.68 \text{ kNm}}{1.00 \cdot 2.00 \cdot 583.4857 \text{ cm}^3 \cdot 355 \text{ MPa}} = 0.1782 \leq 1.00 \quad (8)$$

$$\frac{N_{Ed}}{\chi Af_y} + 0.9 \frac{M_{Ed}}{\gamma_{M1} \cdot \gamma_{frm} \cdot W_{el,min} f_y} = \frac{-218.10 \text{ kN}}{0.5773 \cdot 155 \text{ cm}^2 \cdot 355 \text{ MPa}} + 0.9 \frac{-26.68 \text{ kNm}}{1.10 \cdot 2.00 \cdot 583.4857 \text{ cm}^3 \cdot 355 \text{ MPa}} = 0.1035 \leq 1.00$$

For this case, only 20% of the structural capacity is utilized. As the Viacon Supercor SB-8L is the profile that best fits the space below the existing bridge and there is no thinner version available, no further optimization is possible.

#### 4. Discussion and Conclusions

The bridge presented in this study highlights a typical situation, which can be seen across the country many times. A lot of the bridges that are still operated on the local and national roads have been built in the 1960s and 1970s and were designed for a lifespan

of 50 years. As some of these roads are essential to different areas or human/business activities, traffic cannot be completely interrupted. The only way to repair them is to maintain traffic, even at a reduced/limited level.

The typical solution is to make the necessary repair or reconstruction works on half of the structure or to find a good alternative access nearby. Both of these solutions generate major difficulties for road traffic, which becomes even worse if the road had high values of traffic to start with.

An innovative rehabilitation solution is presented in this paper, which manages to offer the necessary structural support and, at the same time, does not generate more than minor restrictions on the traffic of the crossing road. The paper includes practical aspects, and presents the major challenges and how they were solved both in the design and construction stages.

Placing a corrugated flexible steel structure under the bridge represents an atypical use for this kind of structure, which is normally placed inside a high-quality earth fill that offers support and reduces the risk of buckling. The main challenges of the project and the solutions used are:

- Due to the very little room available between the steel structure and the concrete bridge, the assembly took place on one side and the complete steel structure was slid in its final position;
- Because the earth fill could not be executed between the steel structure and the existing bridge, it was replaced by a monolithic concrete fill; this creates a unique loading situation for this type of structure;
- On the sides of the existing structure, the provisioned extension utilized the classic earth fill solution around the flexible steel structure;
- To minimize stiffness differences on the pavement, a reinforced concrete slab was executed, that rests on the lateral earth fill and is connected to the existing structure and the head wall.

This case study highlights the main advantages this solution has over the classical approaches of retrofitting or demolishing and rebuilding the bridge in the usual concrete solutions:

- Simplified design: apart from the steel structure, which is supplied in full by the factory, there are very few additional details necessary.
- Easy and fast assembly: all steel segments are completely galvanized and all connections are bolted; assembly usually does not extend past a couple of days, even with a small crew.
- Reduces execution time: in comparison with a classical concrete solution, the total execution time is greatly reduced; for this case study, which represents a solution of increased difficulty as far as flexible steel structures go, the complete execution time from start to finish was just 3 months.
- Minimal traffic interference: this innovative solution allowed the construction process to take place with minimal traffic interference, as both traffic lanes were kept open the whole time.
- Cost reduction: the presented solution generated a reduction in cost of about 25% from the alternative of demolishing and rebuilding of the bridge.
- Reduced carbon footprint: by choosing to retrofit the existing structure, instead of simply replacing it with a similar new one, and applying an environmentally friendly solution, the carbon footprint is significantly reduced.
- The world infrastructure incorporates a massive number of roads, railways and bridges. It is essential for the development of our society as it offers mobility and has to be maintained in good shape. For this, it requires constant maintenance and repair works. By systematically applying environmentally friendly solutions such as the one described in this paper, the total reduction in carbon footprint may prove to be quite significant.

- This bridge retrofit solution may be applied in the span ranges where corrugated flexible steel structures are an efficient alternative, which means for spans smaller than 30–40 m. For spans larger than 10–15 m, further in-depth studies regarding the interaction between the steel structure, the concrete fill and the original superstructure are required.
- Future directions of this research will include a detailed full-scale field test of a similar solution, with measurements in all the construction stages. In addition to that, an in-depth optimization of the steel structure and maybe even the creation of a special line of products focused solely on the retrofit of bridges are underway.

**Author Contributions:** Conceptualization, D.N. and C.E.C.; methodology, D.N. and M.C.; software, M.C.; validation, D.N. and C.E.C.; formal analysis, M.C.; investigation, D.N.; resources, D.N. and M.C.; writing—original draft preparation, D.N.; writing—review and editing, M.C. and C.E.C.; visualization, D.N. and M.C.; supervision, C.E.C.; project administration, C.E.C. All authors have read and agreed to the published version of the manuscript.

**Funding:** This research received no external funding.

**Acknowledgments:** The project presented in this paper was realized by ViaCon Romania, with major support from the general design company SC Royal CDV SRL, and the construction company SC Conhidro SRL. We send our regards to the investor DRDP Iasi.

**Conflicts of Interest:** The authors declare no conflict of interest.

## References

1. O'Connor, C. *Roman Bridges*; Cambridge University Press: Cambridge, UK, 1993.
2. Pacheco, P. Multi Span Large Decks—The organic prestressing impact. In *Multi-Span Large Bridges*, 1st ed.; Pacheco, P., Magalhaes, F., Eds.; Taylor & Francis Group: London, UK, 2015; Volume 1, pp. 103–124.
3. Bernini, J.; Fitzsimons, N.; Heierli, W. Overfilled Precast Concrete Arch Bridge Structures. In Proceedings of the 16th Congress of International Association for Bridge and Structural Engineering (IABSE), Lucerne, Switzerland, 18–21 September 2000. [CrossRef]
4. Wakeman, A. The NUCON arch—Plain precast concrete arch system. In *Arch Bridges: Proceedings of the First International Conference on Arch Bridges*, Bolton, UK, 3–6 September 1995; ICE: London, England; pp. 645–652. [CrossRef]
5. Halding, P.S.; Hertz, K.D.; Viebaek, N.E.; Kennedy, A. Assembly and Lifting of Pearl-Chain Arches. In Proceedings of the fib Symposium, Copenhagen, Denmark, 18–20 May 2015.
6. Taylor, S.E.; Robinson, D.; Grattan, S.; Long, A.E.; Gupta, A.; Hogg, I. Monitoring of Monkstown Bridge a Novel Flexi-Arch Bridge System. In Proceedings of the 12th Structural Faults and Repairs International Conference, Edinburgh, UK, 10–12 June 2008.
7. Jeon, S.H.; Cho, K.-I.; Huh, J.; Ahn, J.-H. The Performance Assessment of a Precast, Panel-Segmented Arch Bridge with Outriggers. *Appl. Sci.* **2019**, *9*, 4646. [CrossRef]
8. Jeon, S.H.; Yim, H.J.; Huh, J.; Cho, K.-I.; Ahn, J.-H. Full-scale field testing of a precast concrete buried arch bridge with steel outriggers: Field loading test. *Eng. Struct.* **2021**, *242*, 112563. [CrossRef]
9. Oswald, C.S.; Furlong, R.W. *Observed Behavior of Concrete Arch Culvert*; Research Report No. 932-1F; Center for Transportation Research, The University of Texas at Austin: Austin, TX, USA, 1993.
10. Kay, J.N.; Rigon, C. *Instrumentation of a BEBO Arch Constructed at Byron Bay, New South Wales*; Report No. R77; Department of Civil Engineering, University of Adelaide: Adelaide, Australia, 1986.
11. Beben, D. Interaction of Soil and Bridge Structures Made of Corrugated Steel Plates. Ph.D. Thesis, Faculty of Civil Engineering, Opole University of Technology, Opole, Poland, 2005.
12. El-Taher, M. The Effect of Wall and Backfill Soil Deterioration on Corrugated Metal Culvert Stability. Ph.D. Thesis, Queen's University Kingston, Kingston, ON, Canada, 2009. Available online: <http://hdl.handle.net/1974/5275> (accessed on 1 February 2023).
13. Nakhostin, E.; Kenny, S.; Sivathayalan, S. A numerical study of erosion void and corrosion effects on the performance of buried corrugated steel culverts. *Eng. Struct.* **2022**, *260*, 114217. [CrossRef]
14. Kapliński, O.; Janusz, L. Three phases of multifactor modelling of construction processes. *J. Civ. Eng. Manag.* **2006**, *12*, 127–134. [CrossRef]
15. Beaton, J.L.; Stratfull, R.F. Field test for estimating service life of corrugated metal pipe culverts. In Proceedings of the 41st Annual Meeting of the Highway Research Board, Washington, DC, USA, 1962; Volume 41, pp. 255–272.
16. Hepfner, J.J. *Statewide Corrosivity Study on Corrugated Steel Culvert Pipe (No. FHWA/MT-01-001/8148)*; Montana Department of Transportation. Research, Development and Technology Transfer Program: Montana, Canada, 2002. [CrossRef]
17. Cichocki, R.; Moore, I.; Williams, K. Steel buried structures: Condition of Ontario structures and review of deterioration mechanisms and rehabilitation approaches. *Can. J. Civ. Eng.* **2021**, *48*, 159–172. [CrossRef]

18. White, H.L.; Layer, J.P. The corrugated metal conduit as a compression ring. In Proceedings of the 39th Annual Meeting, Highway Research Board, Washington, DC, USA, 11–15 January 1960.
19. Chen, T.; Su, M.; Pan, C.; Zhang, L.; Wang, H. Local buckling of corrugated steel plates in buried structures. *Thin-Walled Struct.* **2019**, *144*, 106348. [[CrossRef](#)]
20. American Association of State Highway and Transportation Officials (AASHTO) *AASHTO LRFO Bridge Design Specification*; American Association of State Highway and Transportation Officials (AASHTO): Washington, DC, USA, 2017.
21. Transport Canada. *Ontario Highway Bridge Design Code (OHBDC)*; Transport Canada: Toronto, ON, Canada, 2014.
22. Manko, Z.; Beben, D. Research on steel shell of a road bridge made of corrugated plates during backfilling. *J. Bridge Eng.* **2005**, *10*, 592–603. [[CrossRef](#)]
23. Sargand, S.; Masada, T.; Moreland, A. 2008. Measured field performance and computer analysis of large-diameter multiplate steel pipe culvert installed in Ohio. *J. Perform. Constr. Facil.* **2008**, *22*, 390–397. [[CrossRef](#)]
24. Machelski, C. Estimation of internal forces in the shell of soil-steel structures on the basis of its displacements during backfilling. *Stud. Geotechnica et Mech.* **2009**, *31*, 19–38.
25. Manko, Z.; Beben, D. Static load tests of a road bridge with a flexible structure made from Super Cor type steel corrugated plates. *J. Bridge Eng.* **2005**, *10*, 604–621. [[CrossRef](#)]
26. Yeau, K.Y.; Sezen, H.; Fox, P.J. Load performance of in situ corrugated steel highway culverts. *J. Perform. Constr. Facil.* **2009**, *23*, 32–39. [[CrossRef](#)]
27. Bayoglu Flener, E. Testing the response of box-type soil-steel structures under static service loads. *J. Bridge Eng.* **2010**, *15*, 90–97. [[CrossRef](#)]
28. McLean, D.I.; Marsh, M.L. *Dynamic Impact Factors for Bridges*; National Cooperative High-way Research Program, NCHRP Synthesis 266; National Research Council: Washington, DC, USA, 1998.
29. Sezen, H.; Yeau, K.Y.; Fox, P.J. In-situ load testing of corrugated steel pipe-arch culverts. *J. Perform. Constr. Facil.* **2008**, *22*, 245–252. [[CrossRef](#)]
30. Manko, Z.; Beben, D. Dynamic testing of a corrugated steel arch bridge. *Can. J. Civ. Eng.* **2008**, *35*, 246–257. [[CrossRef](#)]
31. Bayoglu Flener, E.; Karoumi, R. Dynamic testing of a soil-steel composite railway bridge. *Eng. Struct.* **2009**, *31*, 2803–2811. [[CrossRef](#)]
32. Beben, D. Dynamic amplification factors of corrugated steel plate culverts. *Eng. Struct.* **2013**, *46*, 193–204. [[CrossRef](#)]
33. Xu, P.; Wei, Y.; Yang, Y.; Zhou, X. Application of fabricated corrugated steel plate in subway tunnel supporting structure. *Case Stud. Constr. Mater.* **2022**, *17*, e01323. [[CrossRef](#)]
34. Cazacu, C.; Negrea, D. Flexible steel structures used for ski tunnels in Parang Mountains, Romania. *IOP Conf. Ser. Mater. Sci. Eng.* **2022**, *1242*, 012026. [[CrossRef](#)]
35. *ACI Committee 347*; ACI 347R-14. Guide to Formwork for Concrete. American Concrete Institute: Farmington Hills, MI, USA, 2014.
36. *EN 1993-1-1:2005*; Eurocode 3: Design of Steel Structures—Part 1-1: General Rules and Rules for Buildings. European Committee for Standardization: Brussels, Belgium, 2005.
37. *EN 1993-2:2006*; Eurocode 3: Design of Steel Structures—Part 2: Steel Bridges. European Committee for Standardization: Brussels, Belgium, 2005.

**Disclaimer/Publisher’s Note:** The statements, opinions and data contained in all publications are solely those of the individual author(s) and contributor(s) and not of MDPI and/or the editor(s). MDPI and/or the editor(s) disclaim responsibility for any injury to people or property resulting from any ideas, methods, instructions or products referred to in the content.